Bader's Electron Density Analysis of Hydrogen Bonding in Secondary Structural Elements of Protein

R. Parthasarathi,[†] S. Sundar Raman,[†] V. Subramanian,*[,†] and T. Ramasami[‡]

Chemical Laboratory, Central Leather Research Institute, Adyar, Chennai 600 020, India, Department of Science and Technology, New Mehrauli Road, New Delhi 110 016, India, and Jawaharlal Nehru Centre for Advanced Scientific Research, Jakkur P. O., Bangalore 560064, India

Received: February 23, 2007; In Final Form: May 11, 2007

The hydrogen-bonding (H-bonding) interactions in α-helical and β-sheet model peptides have been studied by using the atoms-in-molecule (AIM) approach. The relative importance of NH···O and CH···O H-bonding interactions in the different secondary elements such as α-helix, parallel, and antiparallel β-sheets have been assessed. The electron density values at the NH···O bond are higher than those of the CH···O bonds in the α-helical conformation. The electron density values at the H-bonded critical points (HBCPs) corresponding to NH···O and CH···O interactions are nearly equal in the parallel β-sheet of the order of 10^{-3} au, whereas in the case of antiparallel β-sheets, $\rho(r_c)$ values for NH···O and CH···O interactions are of the order of 10^{-2} and 10^{-3} au, respectively. It is interesting to point out here that the weakening of NH···O interactions in the parallel β-sheet arrangement is evident from the AIM analysis. This is concomitant with the increase in the NH···O distance in the parallel β-sheet conformation. In addition to the clear description of H-bonding by electron density at the HBCP, possible good linear relationships between the electron density at ring critical points (RCP) and stabilization energy (SE) have been observed corresponding to the various β-sheet conformations.

Introduction

Studies on hydrogen-bonding (H-bonding) interaction in several model systems have been performed with a view to understand various chemical and biochemical processes in real life systems.[1,2] The interactions between biomolecular systems play an important role in physics, chemistry, and especially in biology. Molecular interactions affect many biochemical processes, for example, molecular recognition. H-bonding interaction between nucleic acid bases is a typical and important example, responsible for the structure and function of DNA and interactions between polypeptides and proteins, which is of key importance for its folding, function, and biological consequences. Hence, the prediction of the structure, energetics, and spectra of such systems is of primary interest in all quantum-chemical calculations.[3] The main goal of quantum chemical calculations is to complement experiments and provide information, predictions, and clear understanding which are not easily accessible by experimental techniques, in order to elucidate the nature of the processes studied.

The construction of complex protein folds relies on the precise conversion of a linear polypeptide chain into a compact 3D structure.[2,4,5] The relationship of the forces that link sequence and folding is intricate and yet to be firmly elucidated. Analysis of 3D structures suggests that complex protein folds consist of a limited number of secondary structural elements, such as strands, helices, and turns, which are assembled using loosely structured loops. With a view to understand the interplay of the forces that connect sequence and protein folding, numerous research works have been carried out in the past.[2,4−7] Since the volume of literature on this topic is massive, it is an extremely difficult task to review here. However, it is necessary to point out that both experimental and theoretical methods have been extensively used to derive the relationship between sequence, structure, folding, and function.[7] The first step in the understanding of the sequence−structure relationship calls for conformational analysis of various amino acids. In this context, Ramachandran's stereochemical plot ($\phi-\psi$ diagram) of dipeptides[8,9] has been widely used to predict the secondary structures of proteins.[7−9] From the point of computational chemistry, both molecular mechanics and molecular dynamics methods have been widely used to understand the structure of polypeptides and proteins. However, rigorous quantum chemical calculations on these systems are limited due to the number of atoms present in the proteins.[10−31] It is important to mention here that high-level ab initio and DFT calculations on polypeptides have been possible only recently.[18−31]

Several theoretical calculations with different levels of accuracy have been made on the polypeptides to study the $\phi-\psi$ plot distribution, H-bonding interactions, and stability.[4−36] In the stability of polypeptides and proteins, the H-bond plays an important role in the formation of secondary structures such as the α-helix, β-sheet, etc., and higher order structures.[33−36] Quantum chemical calculations on some of the secondary structures in proteins/peptides (β-sheets, β and γ turns) at the HF, MP2 levels, and different DFT parametrization schemes have been performed with special emphasis to the H-bonded structures.[13] Most of electronic structure calculations[12−31] have concentrated on the (i) structure, (ii) long-range interaction, (iii) peptide−water interaction, and (iv) electronic properties. These

* Address correspondence to this author. Phone: +91-44-2441-1630. Fax: +91-44-2491-1589. E-mail: subuchem@hotmail.com.
[†] Central Leather Research Institute.
[‡] Department of Science and Technology and Jawaharlal Nehru Centre for Advanced Scientific Research.

10.1021/jp071513w CCC: $37.00
Published on Web 06/28/2007

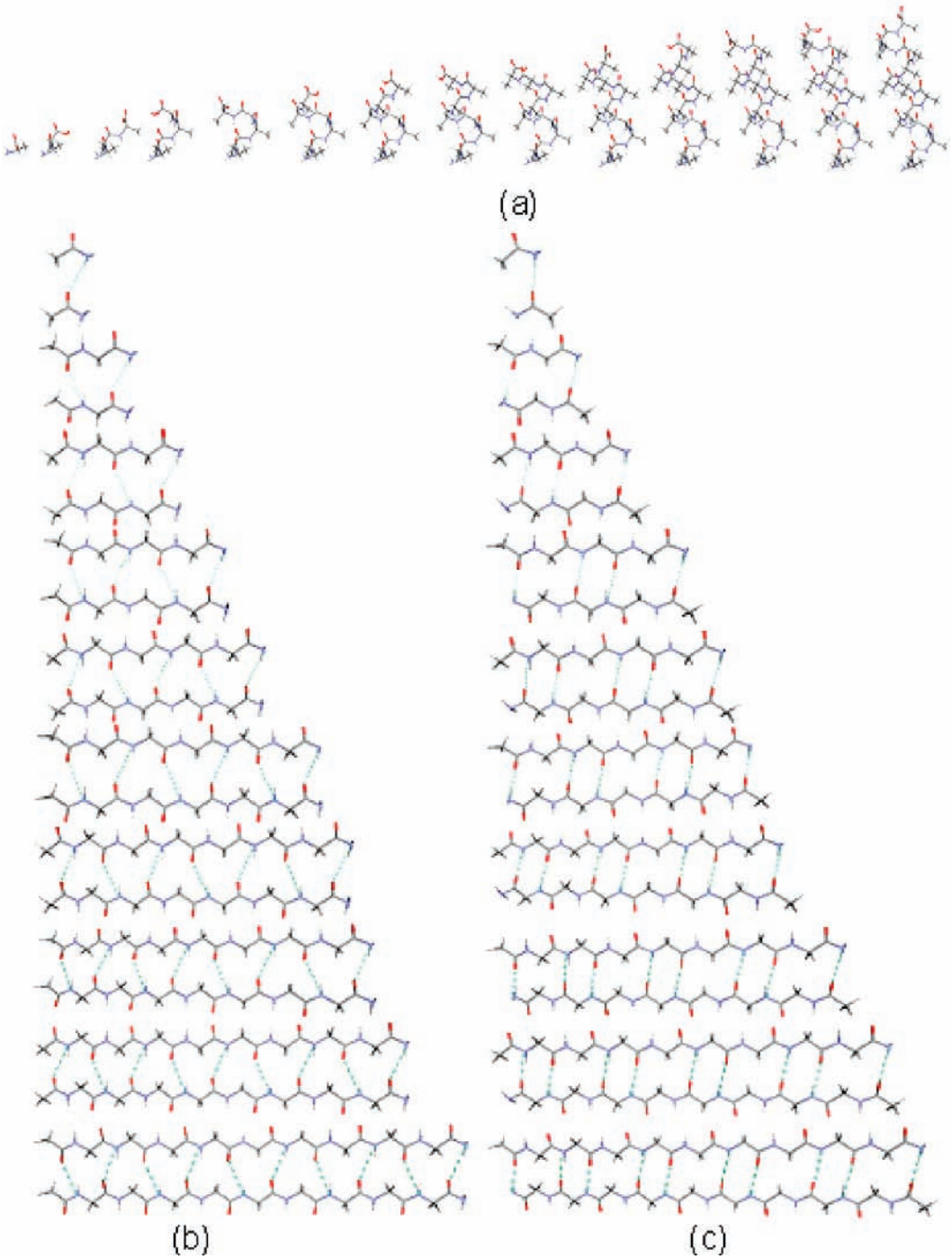

Figure 1. Minimized molecular structure of various (a) α-helical$_{n=1-14}$ (b) parallel β-sheet $_{n=1-10}$, and (c) antiparallel β-sheet$_{n=1-10}$ peptides with H-bonding.

studies have also affirmed the central role played by the H-bonding interactions in protein.

The protein secondary structural elements are stabilized by both inter- and intramolecular H-bonds.[2] Generally CH···O and NH···O H-bonds are mainly responsible for the stabilization of these elements in various proteins.[28,29] The cooperativity of these H-bonds plays a crucial role in the stabilization of protein structure and folding.[25−27,31] Although a number of high-level quantum chemistry calculations have been made on the polypetides, very little information is available on the quantification of various H-bonds in the different secondary structural elements. The understanding and quantification of H-bonds in the various secondary structural elements are necessary to develop a strategy for de nova designing of new folding patterns and foldamers. It is noteworthy to state here that the importance of H-bonding interactions enumerating in various fields has led to the development of necessary and sufficient criteria for H-bonding, which include geometric, energetic, and spectroscopic characteristics.[33−36] In addition, the theory of AIM has been employed to characterize and quantify the H-bonding interaction.[37−46]

The power of AIM theory in elucidating the H-bonded interaction has been discussed on neutral and ionic clusters including citations on the present context.[45,46] The AIM theory has been utilized to determine the C–H···O contacts in A···U Watson–Crick (WC) and U···U base pairs, using nonempirical ab initio calculations.[32] The interaction of hydrated Mg^{2+} cation with bases, base pairs, and nucleotide has been studied with

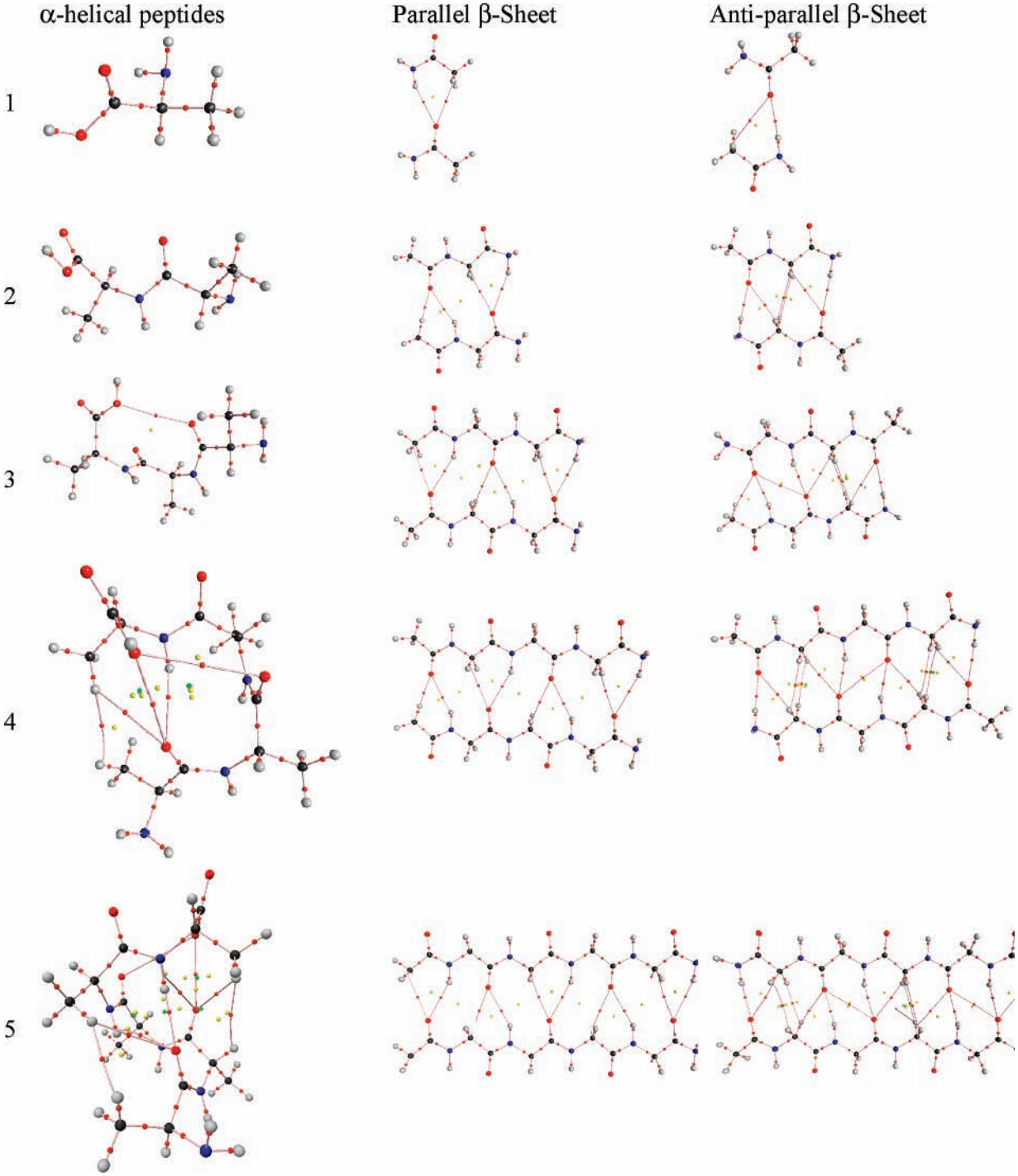

Figure 2. Molecular topography of α-helical, parallel β-sheet, and antiparallel β-sheet peptides as obtained from theoretical electron density.

the help of various theoretical approaches including AIM theory.[38] The topological parameters obtained from this study clearly explained the striking difference in the cation-induced enhancement of base pairing observed in guanine-containing base pairs compared to adenine-containing base pairs. Similarly, the possibility for AIM theory to analyze a polypeptide or a particular portion of a peptide has been described.[11,12,36,45] Previous studies on H-bonding have revealed that such valuable information can be obtained from the electron density analysis.[37,39−46] Prompted by these wide applications and the success of AIM theory, a systematic study has been initiated on a variety of model secondary structural elements of protein to understand and characterize the H-bonding interactions.

Computational Details

The geometries of the α-helix, parallel, and antiparallel β-sheets were constructed by using the biopolymer and model builder modules of the INSIGHT II molecular simulation package (Accelrys, USA).[47] The starting geometries of the peptide models were minimized with the dihedral angles constrained at their ideal values as described by Ramachandran and co-workers[8,9] using the steepest gradient, followed by a conjugate gradient approach employing consistent valence force field (CVFF),[48] using the Discover module (Accelrys, USA). For the α-helix, the poly alanine amino acid sequence has been taken as the representative model $(Ala)_n$ ($n = 1-14$). The

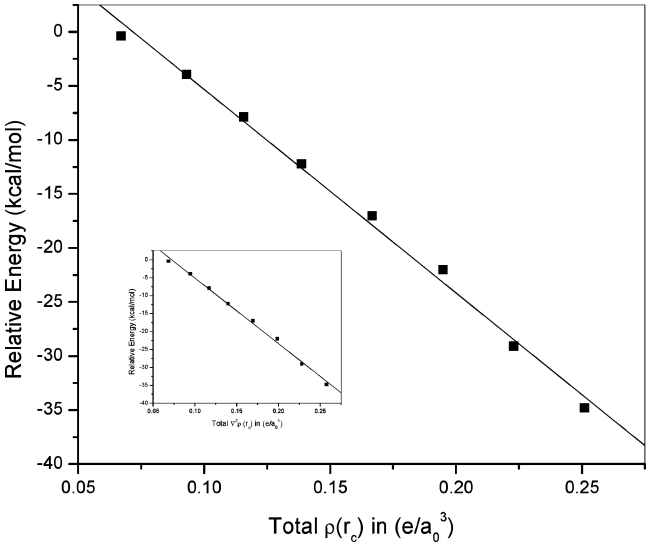

Figure 3. Relationship between relative energy (HF/6-31G*) and total $\rho(r_c)$ and total $\nabla^2\rho(r_c)$ (inset) for α-helical peptides.

backbone torsional angles for the α-helix were set to $\phi = -57.0°$ and $\psi = -47.0°$.[2,7−9] The parallel and antiparallel β-sheets were constrained to be planar ($\phi = \psi = 180°$),[2,7−9] with repeating glycine residues up to $n = 1-10$ units. In the energy minimization, the geometries were then refined until convergence (criterion of the root-mean-square (rms) energy gradient of 0.001 kcal/mol per Å) was reached throughout. These optimized atomic coordinates of ideal α-helix and β-sheet structures were used for quantum chemical calculation without any further optimization. All the ab initio quantum calculations (single point) at the HF/6-31G* level were carried out by using the Gaussian 98W suite program.[49] The wave function generated from the ab initio calculations has been used to generate the electron density topography of polyalanine in α-helix and polyglycine in β-sheet conformations. The AIM calculations were carried out with use of AIM 2000 package.[50]

Calculation of Relative Energies of α-Helix. To quantify the role of H-bonding in the stabilization of α-helix, the total energies of the same sequence in the extended conformation have been obtained from the HF/6-31G* level of calculation. By using the total energy of the same sequence in the α-helix arrangement, the relative energy (RE) has been calculated with the following equation:

$$\mathrm{RE} = E_{\alpha-\text{helical conformatiom}} - E_{\text{Extended conformation}} \quad (1)$$

Calculation of Stabilization Energies of β-Sheets. For both parallel and antiparallel β-sheets, the stabilization energy (SE) was computed by using the following equation, using supermolecular approach

$$\mathrm{SE} = |E_{\text{sheet}} - (E_{\text{peptide1}} + E_{\text{peptide2}})| \quad (2)$$

where E_{sheet}, E_{peptide1}, and E_{peptide2} are the total energies of the β-sheet and individual energies of the interacting peptides obtained from the HF/6-31G* level of calculation. The SE is corrected for BSSE by following the method of Boys and Bernardi.[51]

Results and Discussion

Figure 1 shows the minimum energy structures of α-helix (ala_{1-14}), parallel and antiparallel β-sheets (gly_{1-10}) obtained from force field calculations along with the H-bonding pattern. The representative molecular electron density topographical features obtained from AIM analysis are shown in Figure 2. The red, yellow, and green dots indicate BCP, RCP, and CCP, respectively.

AIM Analysis of H-Bonding in α-Helical Peptides. A complete coverage of recent literature on the theoretical calculation on the α-helix is beyond the scope of this investigation. However, some of the important observations from the quantum chemistry calculations relevant to the present context are discussed here. H-bonding cooperativity and energetics of α-helix formation have been investigated by Wieczorek and Dannenberg.[19,22] The various factors contributing to the stability of α-helix have been summarized in this study. The origin of cooperativity in α-helix formation has been assessed by Morozov et al. and they have confirmed that electron density redistribution accounts for half of the cooperativity.[31] This work has prompted us to look at the electron density analysis of model α-helices.

It can be seen from the molecular graphs that in the α-helix, both N−H···O and C−H···O interactions are present. The existence of HBCPs and corresponding bond paths between *i*th and *i*+4th residues confirm the presence of N−H···O (∼2.1 Å) bonding in the α-helix. This interaction is predominant in the stabilization of the α-helix. In addition, the different atomic interactions are curved and winding in appearance which exemplifying the helical nature present in the chosen model peptides. The number of BCP, HBCP, RCP, CCP, NH···O,

TABLE 1: Number of Bond Critical Points (nBCP), H-bonded Critical Points (nHBCP), Ring Critical Points (nRCP), Cage Critical Points (nCCP), NH···O, CH···O Interactions, Relative Energies, Total Electron Density ($\sum\rho(r_c)$), and Total Laplacian of Electron Density ($\sum\nabla^2\rho(r_c)$) for the α-Helical Peptides

no. of residues	nHBCP	nRCP	nCCP	nN−H···O	nC−H···O	$\sum\rho(r_c)$ (e/a_o^3)	$\sum\nabla^2\rho(r_c)$ (e/a_o^5)	rel energies (kcal/mol)
1	-							
2	-							2.2
3	-	1						4.74
4	2	7	2	1	1	0.0111	0.0132	5.16
5	4	7	2	3	1	0.0281	0.0294	4.53
6	6	22	8	3	3	0.0497	0.0513	2.19
7	7	27	9	4	3	0.067	0.0682	−0.4
8	10	34	12	5	5	0.0931	0.0945	−3.92
9	12	42	14	6	6	0.1157	0.117	−7.87
10	14	49	16	7	7	0.1386	0.1398	−12.2
11	16	56	18	8	8	0.1667	0.1692	−17.0
12	18	62	20	9	9	0.1948	0.1986	−22.0
13	20	69	22	10	10	0.2229	0.228	−29.1
14	22	76	24	11	11	0.251	0.2574	−34.8

TABLE 2: Number of H-bonded Critical Points (nHBCP), Ring Critical Points (nRCP), Stabilization Energies (SE), Stabilization Energies Increment, Total Electron Density ($\sum\rho(r_c)$), and Total Laplacian of Electron Density ($\sum\nabla^2\rho(r_c)$) at HBCP and RCP, Respectively, for the Parallel β-Sheet

no. of residues	nHBCP	nRCP	$\sum\rho(r_c)$ (e/a_o^3) in HBCP	$\sum\nabla^2\rho(r_c)$ (e/a_o^5) in HBCP	$\sum\rho(r_c)$ (e/a_o^3) in RCP	$\sum\nabla^2\rho(r_c)$ (e/a_o^5) in RCP	SE (kcal/mol)	SE increment (kcal/mol)
1	2	1	0.012	0.0131	0.004	0.005	3.83	3.83
2	4	3	0.035	0.0369	0.011	0.0133	7.64	3.8
3	6	5	0.036	0.0395	0.014	0.0178	11.4	3.72
4	8	7	0.059	0.0633	0.02	0.0261	15	3.64
5	10	9	0.059	0.0659	0.024	0.0307	19.1	4.1
6	12	11	0.083	0.0906	0.03	0.039	22.8	3.69
7	14	13	0.082	0.0923	0.033	0.0435	27	4.2
8	16	15	0.105	0.116	0.04	0.0518	30.7	3.71
9	18	17	0.105	0.1185	0.043	0.0563	35	4.26
10	20	19	0.147	0.1603	0.053	0.069	38.7	3.72

TABLE 3: Number of H-bonded Critical Points (nHBCP), Ring Critical Points (nRCP), Stabilization Energies (SE), Stabilization Energies Increment, Total Electron Density ($\sum\rho(r_c)$), and Total Laplacian of Electron Density ($\sum\nabla^2\rho(r_c)$) at HBCP and RCP, Respectively, for the Antiparallel β-Sheet

no. of residues	nHBCP	nRCP	$\sum\rho(r_c)$ (e/a_o^3) in HBCP	$\sum\nabla^2\rho(r_c)$ (e/a_o^5) in HBCP	$\sum\rho(r_c)$ (e/a_o^3) in RCP	$\sum\nabla^2\rho(r_c)$ (e/a_o^5) in RCP	SE (kcal/mol)	SE increment (kcal/mol)
1	2	1	0.018	0.0182	0.005	0.0054	4.5	4.5
2	4	5	0.036	0.037	0.017	0.0184	15.4	10.9
3	6	9	0.06	0.0597	0.032	0.0374	15.7	0.34
4	8	14	0.085	0.0858	0.048	0.0544	26.5	10.8
5	10	17	0.105	0.1062	0.06	0.0698	26.1	−0.45
6	12	22	0.121	0.1212	0.076	0.087	36.8	10.7
7	14	23	0.142	0.1417	0.082	0.0956	36	−0.72
8	16	29	0.162	0.1622	0.103	0.1193	45.9	9.87
9	18	28	0.183	0.1827	0.102	0.1195	46	0.03
10	20	34	0.204	0.2032	0.126	0.147	56.9	10.9

CH···O interactions, relative energies, total $\rho(r_c)$, and total $\nabla^2\rho(r_c)$ at the HBCPs for the α-helical peptides are summarized in Table 1. The relative energies for various polyalanine sequences show that at least 7 residues are necessary for the formation of stable α-helical conformation. It can be seen from the relative energy that the addition of one alanine residue to the $(Ala)_7$ is 3.88 kcal/mol. As the length of the helical sequence increases, the relative stability increases. It is interesting to observe that addition of one alanine residue increases the stability due to H-bonding cooperativity as reported in the previous studies.[19,22] The values of $\rho(r_c)$ and $\nabla^2\rho(r_c)$ at these points are typically of the order of 10^{-2} and 10^{-3} au, respectively, which are similar to the values stipulated for the H-bonding by Bader and coworkers.[37] The Laplacian of electron density is also positive confirming the presence of H-bonded interactions.

The $\rho(r_c)$ values at the HBCPs corresponding to the C−H···O interactions are marginally lower than that of N−H···O H-bonds. It is interesting to note that electron density analysis clearly portrays the relative importance of these two H-bonded interactions in the stabilization of helical motif. It is well-known that about one-fourth of amino acid residues in polypeptides are found in α-helical conformation. However, the exact fraction varies with the one protein to the other. The preference of amino acid residues to form α-helical conformation mainly arises due to the fact that the α-helix optimally uses the intramolecular H-bonds for its stability. Every peptide bond participates in the H-bonding interaction in the formation of the helix, which is accurately reinforced by the presence of HBCPs.

TABLE 4: Electron Density Values ($\rho(r_c)$) of NH···O and CH···O H-Bonds in Parallel and Antiparallel β-Sheets$_{(n=5)}$

H-bond	$\rho(r_c)$ (e/a_o^3) parallel	$\rho(r_c)$ (e/a_o^3) antiparallel
CH···O	0.0066	0.0051
NH···O	0.0053	0.0143
CH···O	0.0065	0.0052
NH···O	0.0052	0.0147
CH···O	0.0064	0.0051
NH···O	0.0053	0.0148
CH···O	0.0065	0.0053
NH···O	0.0052	0.0152
CH···O	0.0064	0.0055
NH···O	0.0056	0.0152

It can be seen from Table 1 that the sum of the electron density at the HBCPs increases as the stability of the helix increases. It also can be seen that the Laplacian of the electron density follows a similar trend. In the stabilization of the helix, the microdipole of the peptide bonds plays an important role. Each microdipole is connected through the intramolecular H-bonding and results in a net dipole extending down the helix, which increases with helix length. The linear relationship between the relative energies and the sum of electron density and its Laplacian at the HBCPs is shown in Figure 3. The AIM theory helps to characterize the strength of interaction between the two dipoles in the helical chain. Similar to the microdipole of the peptide bond, the sum of electron density values at the N−H···O and C−H···O HBCPs exhibits a direct relationship with the relative energy and hence its stability. The linear regression analysis yields

$$\mathrm{RE} = -188.35\rho(r_c) + 13.5, \quad R = -0.99 \qquad (3)$$

$$\mathrm{RE} = -183.07\nabla^2\rho(r_c) + 13.2, \quad R = -0.99 \qquad (4)$$

AIM Analysis of H-Bonded Parallel and Antiparallel β-Sheets. Recently, several interesting theoretical calculations have been made on the β-sheet models.[18,21,24−28] Horvath et al. have studied the long-range effects in the formation of β-sheet structure.[26] This study brought out the considerable role played

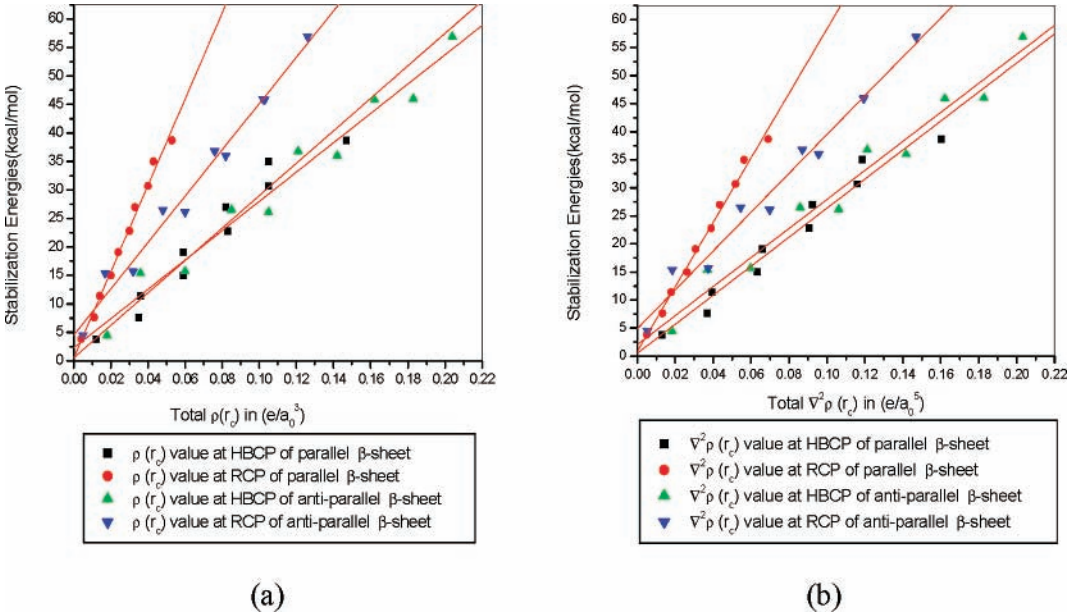

Figure 4. Relationship between SE (HF/6-31G*) and (a) total $\rho(r_c)$ and (b) total $\nabla^2\rho(r_c)$ for parallel and antiparallel β-sheets.

by the long-range interactions in the stabilization of the β-sheet model (Gly_{10}). The question of network cooperativity in the model β-sheets has been addressed by Zhao et al.[27] The interplay between network cooperativity and electrostatics has been highlighted in these model systems.[27] Scheiner and co-workers have made extensive investigation on the assessment of contribution of NH···O and CH···O H-bonds using ab initio quantum chemical calculations.[28,29] Both geometric and energetic analyses have been carried out. It is found that NH···O and CH···O approximately and equally contribute to the stability of interstrand binding energy. Earlier work on various model β-sheets provided a similar conclusion. However, the exact difference between these two interactions is not quantified. In this connection, AIM theory becomes versatile and provides a possible means to disentangle the contribution made by these two types of H-bonded interactions.

The number of HBCP, RCP, SE, incremental SE, total $\rho(r_c)$, and total $\nabla^2\rho(r_c)$ at HBCP and RCP, respectively, for the parallel and antiparallel β-sheet are listed in Tables 2 and 3. It can be seen from the energetics of parallel β-sheets that incremental SE ranges from 3.64 to 4.26 kcal/mol. There is no dramatic change in the SE upon addition of one glycine residue in the parallel sheet conformation. However, in antiparallel β-sheets, it is possible to observe a significant variation in the trend of incremental SEs. In these systems, odd- and even-numbered residues contribute to the stability in a different fashion. The second, fourth, sixth, and the other even-numbered systems form large H-bonded rings (LHRs) and hence higher SE. The third, fifth, and odd-numbered sheet structures form smaller H-bonded ring (SHR) structures and cause destabilization. This behavior has also been observed in the recent study on β-sheet models.[27] For parallel and antiparallel β-sheets, electron density topography features are shown in Figure 2. The electron density topography features clearly reveal the formation of LHR and SHR in the model β-sheets. It is possible to note from the molecular graph that intermolecular H-bonding between the two chains is evident and these topography parameters are also in the range set by Bader's theory.[37]

The values of electron density at the HBCPs and associated topographical features clearly discriminate the nature of the primary and secondary interactions found in the basic building blocks of proteins. The cooperativity and long-range effects of H-bonding interactions in the secondary structural elements of protein can be explained by electron density topography analysis. One of the primary motives of the present study is to gain insight into the difference between the strength of NH···O and CH···O in the stabilization of β-sheets. In the case of antiparallel sheets, the $\rho(r_c)$ values at the HBCPs for the NH···O interaction are marginally higher than those at the HBCPs corresponding to CH···O, and hence the greater stability of antiparallel sheets. On the contrary, for the parallel sheets, there is not much of a difference in the $\rho(r_c)$ values at HBCPs for CH···O and NH···O interactions. In the earlier studies, differences in the geometry of these H-bonding patterns have been attributed to the respective stability. The longer NH···O ($\sim$2.6 Å) bonds in the parallel arrangement immediately suggest weakening of these interactions as a potential source of lower SE. However, the NH···O H-bonds deviate less from the linearity than those of the CH···O bonds. Comparison of geometrical characteristics of NH···O interaction in the parallel and antiparallel arrangements reveals that these bonds are considerably longer in the parallel case, while they are shorter in the antiparallel case ($\sim$2.1 Å). Electron density values of NH···O and CH···O H-bonds in parallel and antiparallel β-sheets$_{(n=5)}$ are reported in Table 4 as a representative example. The analysis of electron density values at different HBCPs for both arrangements shows that NH···O bonds are stronger than the CH···O bonds in the antiparallel arrangement whereas both NH···O and CH···O bonds have

TABLE 5: Regression Equations for Stabilization Energies (SE), Using Total $\rho(r_c)$ and Total $\nabla^2\rho(r_c)$ at H-Bonded Critical Points (HBCP) and Ring Critical Points (RCP) for Parallel and Antiparallel β-Sheets

	HBCP	*R*	RCP	*R*
parallel β-sheet	$SE = 284.6\rho(r_c)_{HBCP} + 0.54$	0.97	$SE = 756.7\rho(r_c)_{RCP} + 0.54$	0.99
	$SE = 258.1\nabla^2\rho(r_c)_{HBCP} + 0.51$	0.98	$SE = 574.9\nabla^2\rho(r_c)_{RCP} + 0.85$	0.99
antiparallel β-sheet	$SE = 257.2\rho(r_c)_{HBCP} + 2.27$	0.98	$SE = 406.6\rho(r_c)_{RCP} + 4.5$	0.99
	$SE = 258.8\nabla^2\rho(r_c)_{HBCP} + 2.1$	0.98	$SE = 346.1\nabla^2\rho(r_c)_{RCP} + 4.9$	0.99

nearly equal strength in the parallel sheets in accordance with the earlier findings. The weakening of NH···O interactions in the parallel sheets is also observed from the electron density values at the HBCPs. The relationships between the sum of the electron density values and its Laplacian at all HBCPs vs the SE of both sheets have been studied and the same has been presented in Figure 4. The linear regression equations are presented in Table 5. An excellent linear relationship between the SE and the sum of electron density values shows that both NH···O and CH···O are important in the stabilization of sheets and relative significances of NH···O and CH···O interactions can be assessed from the electron density values at the HBCPs. In addition, these equations can be used in the quantitative structure activity (QSAR) parlance to predict the stability of larger helical and sheet structure of synthetic peptides and natural protein sequences, using the average values of electron density at NH···O and CH···O HBCPs.

However, in addition to the H-bonding interaction, it is evident that other secondary interactions also lead to further stability. Rich electron density topography features can be observed from the molecular graphs depicted in Figure 2 corresponding to parallel and antiparallel β-sheets. It is evident from the geometry of the β-sheets that it exhibits H-bonded, large and small ring structures. The importance of these H-bonded rings in the stabilization of β-sheet structures has been discussed in a previous report.[27] To quantify these rings in the parallel and antiparallel sheets, the relationship between the electron density values at the ring critical point (RCP) and SE has been probed. In this study, an attempt has been made to probe the RCP to illustrate the clear depiction of the interactions. The linear relationship presented in Figure 4 clearly displays the role of ring structure in the stabilization of sheet structures. It is interesting to note from parts a and b of Figure 4 that the $\rho(r_c)_{RCP}$ and $\nabla^2\rho(r_c)_{RCP}$ respectively show a good linear relationship with the SE of both parallel and antiparallel β-sheets. The corresponding linear fits for SE vs $\rho(r_c)_{RCP}$ and SE vs $\nabla^2\rho(r_c)_{RCP}$ are given in Table 5.

The analysis of the topographical features of the β-sheets clearly provides the possible reasons for the observed results. It is evident from the electron density topographical features of β-sheets that the variation in the values of HBCP at NH···O and CH···O interaction changes due to the corresponding variation in geometries. However, values of the RCP do not vary during different interactions and hence the possible good linear relationships between the electron density at the RCP and SE corresponding to the various β-sheet conformations. In addition to the electron density properties at the HBCP, the same at RCP also correspond with the stabilization of both sheets at various lengths.

Conclusions

In summary, the electron density topography features are quite useful in delineating and quantifying the H-bonded interaction in the various protein secondary structural elements. The values of $\rho(r_c)$ at the HBCPs clearly distinguish the importance of NH···O and CH···O interaction in the α-helix and β-sheets. It is possible to unravel the importance of NH···O and CH···O interactions in the parallel and antiparallel β-sheets. In the case of the parallel β-sheet, NH···O is weaker than CH···O whereas in the antiparallel sheets, NH···O is stronger than CH···O. In addition, RCPs clearly explains the role of ring structures in the stabilization of sheets. The relationship developed between SE and $\rho(r_c)$ at the HBCPs can be used to predict the stability of synthetic peptides and protein by using the average values of $\rho(r_c)$ at the HBCPs.

Acknowledgment. We acknowledge DST and CSIR, Government of India, New Delhi for financial support. R.P. and V.S. acknowledge the support under DST-DAAD project and Prof. Dr. Gereon Niedner-Schatteburg, TU Kaiserslautern, Germany for his kind help during the visit and collaboration.

References and Notes

(1) Saenger, W. *Principles of Nucleic Acid Structure*; Springer-Verlag: New York, 1984.
(2) Schulz, G. E.; Schirmer, R. H. *Principles of Protein Structure*; Springer-Verlag: New York, 1979.
(3) Hobza. P.; Sponer, J. *Chem. Rev.* **1999**, *99*, 3247.
(4) DeGrado, W. F.; Summa, C. M.; Pavone, V.; Nastri, F.; Lombardi, A. *Annu. Rev. Biochem.* **1999**, *68*, 779.
(5) Venkatraman, J.; Shankaramma, S. C.; Balaram, P. *Chem. Rev.* **2001**, *101*, 3131.
(6) Fersht, W. H. A. *Structure and Mechanism in Protein Science*: *A Guide to Enzyme Catalysis and Protein Folding*; W. H. Freeman and Company: New York, 1999.
(7) Pullman, B.; Pullman, A. *Advances in Protein Chemistry*; Academic Press: New York, 1974.
(8) Ramachandran, G. N.; Ramakrishnan, C.; Sasisekharan, V. *J. Mol. Biol*. **1963**, *7*, 95.
(9) Ramachandran, G. N.; Sasisekharan, V. *Advances in Protein Chemistry*; Academic Press: New York, 1974; Vol. 23, p 283.
(10) Head-Gordon, T.; Head-Gordon, M.; Frisch, M. J.; Brooks, C. L.; Pople, J. A., III *J. Am. Chem. Soc*. **1991**, *113*, 5989.
(11) Chang, C.; Bader, R. F. W. *J. Phys. Chem*. **1992**, *96*, 1654.
(12) Popelier, P. L. A.; Bader, R. F. W. *J. Phys. Chem.* **1994**, *98*, 4473.
(13) Moehle, K.; Gussmann, M.; Rost, A.; Cimiraglia, R.; Hofmann, H.-J. *J. Phys. Chem. A* **1997**, *101*, 8571.
(14) Aleman, C. *J. Phys. Chem. A* **2001**, *105*, 6717.
(15) Wu, X.; Wang, S. *J. Phys. Chem. B* **2001**, *105*, 2227.
(16) Morozov, A. V.; Kortemme, T.; Baker, D. *J. Phys. Chem. B* **2003**, *107*, 2075.
(17) Gnanakaran, S.; Garcia, A. E. *J. Phys. Chem. B* **2003**, *107*, 12555.
(18) Torrent, M.; Mansour, D.; Day, E. P.; Morokuma, K. *J. Phys. Chem. A* **2001**, *105*, 454.
(19) Wieczorek, R.; Dannenberg, J. J. *J. Am. Chem. Soc*. **2003**, *125*, 14065.
(20) Wu, Y. D.; Zhao, Y. L. A. *J. Am. Chem. Soc*. **2001**, *123*, 5313.
(21) Jang, S.; Shin, S.; Pak, Y. *J. Am. Chem. Soc.* **2002**, *124*, 4976.
(22) Wieczorek, R.; Dannenberg, J. J. *J. Am. Chem.* Soc. **2003**, *125*, 8124.
(23) Liu, D.; Wyttenbach, T.; Barran, P. E.; Bowers, M. T. *J. Am. Chem. Soc*. **2003**, *125*, 8458.
(24) Bour, P.; Keiderling, T. A. *J. Mol. Struct.* (*Theochem*) **2004**, *675*, 95.
(25) Wieczorek, R.; Dannenberg, J. J. *J. Am. Chem. Soc*. **2004**, *126*, 14198.
(26) Horvath, V.; Varga, Z.; Kovacs, A. *J. Phys. Chem. A* **2004**, *108*, 6869.
(27) Zhao, Y.-L.; Wu, Y.-D. *J. Am. Chem. Soc*. **2002**, *124*, 1570.
(28) Scheiner, S. *J. Phys. Chem. B* **2006**, *110*, 18670.
(29) Scheiner, S.; Kar, T.; Pattanayak, J. *J. Am. Chem. Soc.* **2002**, *124*, 13257.
(30) Abramavicius, D.; Zhuang, W.; Mukamel, S. *J. Phys. Chem. B* **2004**, *108*, 18034.
(31) Morozov, A. V.; Tsemekhman, K.; Baker, D. *J. Phys. Chem. B* **2006**, *110*, 4503.
(32) Hobza, P.; Sponer, J.; Cubero, E.; Orozco, M.; Luque, F. J. *J. Phys. Chem. B* **2000**, *104*, 6286.
(33) Jeffrey, G. A.; Saenger, W. *Hydrogen Bonding in Biology and Chemistry*; Springer-Verlag: Berlin, Germany, 1991.
(34) Jeffrey, G. A. *An Introduction to Hydrogen Bonding*; Oxford University Press: New York, 1997.
(35) Scheiner, S. *Hydrogen Bonding. A Theoretical Perspective*; Oxford University Press: Oxford, UK, 1997.
(36) Desiraju, G. R.; Steiner, T. *The Weak Hydrogen Bond in Structural Chemistry and Biology*; Oxford University Press: Oxford, UK, 1999.
(37) Bader, R. F. W. *Atoms in Molecules*: *A Quantum theory*; Clarendon: Oxford, UK, 1990.
(38) Munoz, J.; Sponer, J.; Hobza, P.; Orozco, M.; Luque, F. J. *J. Phys. Chem. B* **2001**, *105*, 6051.
(39) Grabowski, S. J. *J. Mol. Struct.* **2001**, *562*, 137.
(40) Grabowski, S. J.; Sokalski, W. A.; Leszczynski, J. *J. Phys. Chem. A* **2005**, *109*, 4331.
(41) Grabowski, S. J.; Sokalski, W. A.; Dyguda, E.; Leszczynski, J. *J. Phys. Chem. B* **2006**, *110*, 6444.
(42) Parthasarathi, R.; Amutha, R.; Subramanian, V.; Nair, B. U.; Ramasami, T. *J. Phys. Chem. A* **2004**, *108*, 3817.

(43) Parthasarathi, R.; Subramanian, V.; Sathyamurthy, N. *J. Phys. Chem. A* **2005**, *109*, 843.

(44) Parthasarathi, R.; Subramanian, V. *Struct. Chem.* **2005**, *16*, 243.

(45) Parthasarathi, R.; Subramanian, V. In *Hydrogen Bonding−New Insight, Challenges and Advances in Computational Chemistry and Physics Series*; Grabowski, S. J., Ed.; Kluwer: New York, 2006; p 1.

(46) Parthasarathi, R.; Subramanian, V.; Sathyamurthy, N. *J. Phys. Chem. A* **2006**, *110*, 3349.

(47) *InsightII, Modeling Environment*; Release 2000.1 ed.; Accelrys Inc.: San Diego, CA, 2001.

(48) Dauber-Osguthorpe, P.; Roberts, V. A.; Osguthorpe, D. J.; Wolff, J.; Genest, M.; Hagler, A. T. *Proteins* **1988**, *4*, 31.

(49) Frisch, M. J.; Trucks, G. W.; Schlegel, H. B.; Scuseria, G. E.; Robb, M. A.; Cheeseman, J. R.; Zakrzewski, V. G.; Montgomery, J. A., Jr.; Stratmann, R. E.; Burant, J. C.; Dapprich, S.; Millam, J. M.; Daniels, A. D.; Kudin, K. N.; Strain, M. C.; Farkas, O.; Tomasi, J.; Barone, V.; Cossi, M.; Cammi, R.; Mennucci, B.; Pomelli, C.; Adamo, C.; Clifford, S.; Ochterski, J.; Petersson, G. A.; Ayala, P. Y.; Cui, Q.; Morokuma, K.; Rega, N.; Salvador, P.; Dannenberg, J. J.; Malick, D. K.; Rabuck, A. D.; Raghavachari, K.; Foresman, J. B.; Cioslowski, J.; Ortiz, J. V.; Baboul, A. G.; Stefanov, B. B.; Liu, G.; Liashenko, A.; Piskorz, P.; Komaromi, I.; Gomperts, R.; Martin, R. L.; Fox, D. J.; Keith, T.; Al-Laham, M. A.; Peng, C. Y.; Nanayakkara, A.; Challacombe, M.; Gill, P. M. W.; Johnson, B.; Chen, W.; Wong, M. W.; Andres, J. L.; Gonzalez, C.; Head-Gordon, M.; Replogle, E. S.; Pople, J. A.; *Gaussian 98*, Revision A.11.2; Gaussian, Inc.: Pittsburgh, PA, 2001.

(50) Biegler-Konig, F.; Schonbohm, J.; Derdau, R.; Bayles, D.; Bader, R. F. W. *AIM 2000*, Version 1; Bielefeld, Germany, 2000.

(51) Boys, S. F.; Bernardi, F. *Mol. Phys.* **1970**, *19*, 553.